1. Amina BAGDAOUI[1], 2. Zouaoui CHAMA[1], 3. Belkacem HACHEMI[1,2], 4. BOURENNANE EL-BAY[3]

Department of Electronics, University of Djillali Liabes in Sidi Bel Abbes, Algeria (1)
Centre de Développement des Téchnologies Avancées, Algiers, Algeria (2)
ImVia Laboratory, Université de Bourgogne, France (3)

doi:10.15199/48.2024.06.08

Automatic Multi-Segmentation Method for Tumor Detection in MRI Images using Constrained kmeans Method and Region Growing-Quasi Monte Carlo Method

Abstract. *Magnetic Resonance Imaging (MRI) has become an indispensable tool in the medical field, enabling the detection of critical abnormalities affecting various organs within the human body. Despite its inherent complexity, the development of automated or semi-automated detection and recognition techniques has made significant strides. In this paper, we present an innovative approach for the automatic multi and full segmentation of tumor regions within MRI scans. An enhanced region-growing method founded on the Quasi-Monte Carlo sampling and constrained k-means algorithm is presented in this paper, we define distinct classes to facilitate precise segmentation. The efficacy of our technique is evaluated through a range of metrics, demonstrating its robust performance. The proposed fully automated multi-segmentation method showcases superior results and holds potential to supplant conventional techniques for tumor detection in MRI images.*

Streszczenie. *Rezonans magnetyczny (MRI) stał si ¸e niezast ¸apionym narz ¸edziem w medycynie, umo ˙zliwiaj ¸acym wykrycie krytycznych niepraw-idłowo ´sci wpływaj ¸acych na ró ˙zne narz ¸ady w organizmie człowieka. Pomimo swojej nieodł ¸acznej zło ˙zono ´sci, rozwój zautomatyzowanych lub półautomatycznych technik wykrywania i rozpoznawania poczynił znaczne post ¸epy. W artykule przedstawiamy innowacyjne podej ´scie do automatycznej wieloi pełnej segmentacji obszarów nowotworowych w obrazach MRI. W artykule przedstawiono ulepszon ¸a metod ¸e powi ¸ekszania regionów opart ¸a na próbkowaniu Quasi-Monte Carlo i ograniczonym algorytmie k- ´srednich. Definiujemy odr ¸ebne klasy, aby ułatwi ´c precyzyjn ¸a segmentacj ¸e. Skuteczno ´s ´c naszej techniki ocenia si ¸e za pomoc ¸a szeregu wska ´zników, co pokazuje jej solidne działanie. Proponowana w pełni zautomatyzowana metoda wielosegmentacyjna zapewnia doskonałe wyniki i mo ˙ze zast ¸api ´c konwencjonalne techniki wykrywania nowotworów na obrazach MRI. (**Automatyczna metoda wielosegmentacyjna do wykrywania nowotworu w obrazach MRI przy użyciu metody ograniczonych kmean i metody Quasi Monte Carlo wzrostu regionu**)*

Keywords: Brain tumor, Multi Segmentation,Region growing constrained k-means, Quasi Monte carlo, naive Baye.
Słowa kluczowe: Guz mózgu, wielosegmentacja, rosn ¸ace w regionie ´srednie bayesowskie k, Quasi Monte Carlo.

Introduction

Magnetic Resonance Imaging (MRI) has revolutionized medical diagnosis and treatment by enabling non-invasive visualization of internal structures. Detecting abnormalities in organs is crucial for timely medical interventions. Automation of this process has gained prominence due to the sheer volume and complexity of MRI data. This paper introduces an automatic method for the multi-segmentation of tumor regions in MRI scans, leveraging an innovative combination of the quasi-Monte Carlo method and the Expectation Maximization algorithm. MRI segmentation can be done using three different methods, such as manual, semi-automatic and full automatic techniques [6]. For manual MRI segmentation, which is the most common technique, the segmentation is done by a doctor or an expert, and its accuracy depend on the performance and the knowledge of the doctor. Full automatic segmentation technique is an autonomous process and which need evolved algorithms for calculation and recog- nition. Medical image processing methods, used for full automatic segmentation, are classified into four main categories [6, 15]: Threshold based techniques, such as otsu and kapur thresholding, and adaptive thresholding [13] The second category is the region-based technique, such as region growing [9] and watershed [11] Third, the classification techniques that need a training phase, such as SVM and KNN and clustering methods, such as K-means and EM mixture [6] The last category is contour detection, such as ACM, GVF, VFC [16] and level set [1]. Many researchers have presented full automatic and hybridized MRI image segmentation model. Lu et al. [9] used an improved region growing algorithm initialized by the QMC method for liver segmentation. In their turn, W. Y. Zhanfang, and Hongbiao [19] used an improved PCNN method to perform automatic segmentation, however, their method was not applied for the segmented more complex areas. Kuwazuru et al. [8] used hybrid method by combining ANN with the level-set method for segmentation of multiple sclerosis lesion (MS) of the brain. Their method is based on a concatenation. of ANN and level set, but their method was unable to detect small areas. D. Veloz, and Allende [4] used modified EM to segment MRI images. In this paper, we employed enhancement and denoising filters to preprocess the image. Subsequently, we used the Kapur thresholding method to locate the region of interest (ROI). Then, we applied the quasi Monte Carlo method to generate a large number of seeds (Quasi Random Sampling). These seeds were grouped into k classes using an improved version of the K-means method, referred to as constrained K-means, where the spatial dependency of the samples is taken into account. The classification is established within a Naive Bayesian framework. After selecting the optimal seed for each cluster, we initialize our improved region growing approach.

Method

0.1 Preprocessing

As depicted in Figure 1, our approach is structured around three primary stages: preprocessing, localization, and segmentation and recognition. Initially, we employed the deformable model proposed by Rifai et al. [14] to remove the skull. Subsequently, we applied contrast enhancement to accentuate high-frequency regions using sigmoid filtering, as outlined in the work by Lu et al. [9]. The sigmoid filter modifies the distribution of gray levels to enhance dissimilarities between neighboring regions. The gray level of the resulting image is calculated using the equation:

$$p' = (I_{max} - I_{min}) = \frac{1}{1 + \exp\left(-\frac{p + \beta}{\alpha}\right)} + I_{min}$$

Here, p signifies the gray level of the input image, Imax and I_{min} represent the maximum and minimum gray levels of the output image, respectively. α corresponds to the width of the intensity range of the input image, and β indicates the central point of this range.

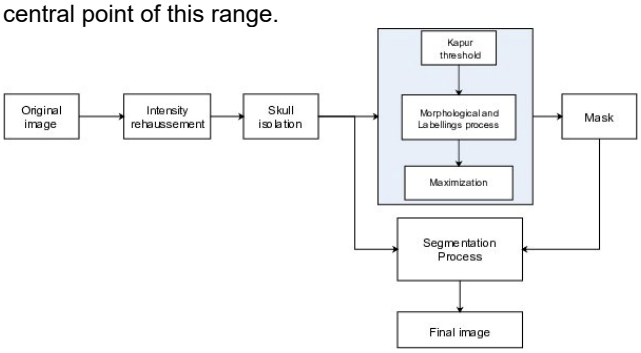

Fig.1. Overview flowchart of image preprocessing

Subsequently, we employed the thresholding method based on the Kapur algorithm [13] to isolate the tumor region, which stands out due to its enhanced color. We computed the entropies of the object H_{ROI} and the background H_{Bg} using the following equations:

$$H_{ROI}(t) = \sum_{i=0}^{t} \frac{\Pr(p_i)}{\Pr(ROI)} \ln\left(\frac{\Pr(p_i)}{\Pr(ROI)}\right)$$

$$H_{Bg}(t) = \sum_{i=0}^{t} \frac{\Pr(p_i)}{\Pr(Bg)} \ln\left(\frac{\Pr(p_i)}{\Pr(Bg)}\right)$$

where $\Pr(ROI) = \sum_{i=0}^{t} P_r(p_i)$, $\Pr(Bg) = \sum_{i=0}^{+\infty} P_r(p_i)$ and $\Pr(ROI) + \Pr(Bg) = 1$ represents the threshold value at the maximum values of H_{ROI} (t) and H_{Bg}(t).

Next, we applied morphological processing to decrease the number of connected regions. Afterward, we labeled regions consisting of connected pixels and identified the region with the highest pixel count as the Region of Interest (ROI).

0.2 Segmentation

In this section, we introduce a new segmentation approach comprised of three pivotal steps, which is an improved iteration of the method proposed in [23]. The initial step involves seed generation, followed by seed clustering into k-classes in the subsequent step. Ultimately, the multi-segmentation is executed after the optimal seeds are selected. The segmentation procedure is visually depicted in Figure 2. The strength of the constrained k-means method lies in its capacity to consider neighboring pixels during the classification process, in contrast to the EM algorithm. This characteristic contributes to a more homogeneous classification. The objective of the Quasi Monte Carlo method is to generate a discrepancy sequence of pixels L in our Region (ROI). To ensure the good coverage of the ROI, we generated the sequence in a rectangle (referenced as RECT) that covers the area and which has the following parameters

$$x_{min} = \min(\text{row}) \quad x_{max} = max(row)$$

$$y_{min} = min(col) \quad y_{max} = \max(\text{col})$$

Where *row* and *col* are, respectively, the Cartesian coordinate vectors of the mask ROI. the Halton sequence was adopted to generate the points with:

$$x_i = [x_{min} + [(x_{max} - x_{min})] \times h_2$$

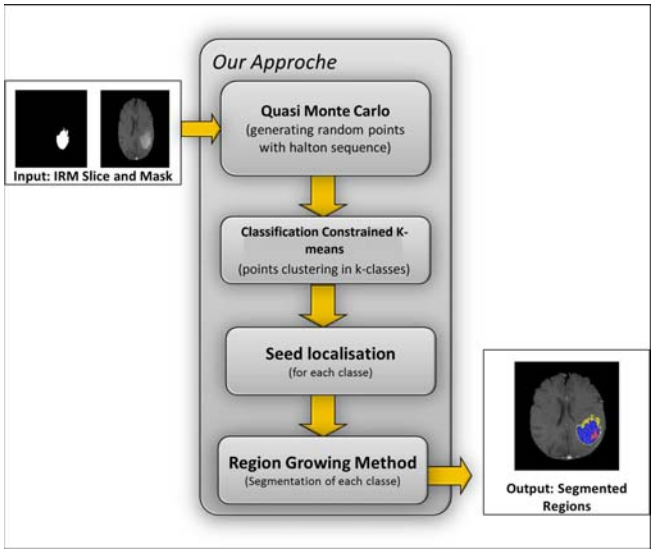

Fig. 2: segmentation flowchart

$$y_i = [y_{min} + [(y_{max} - y_{min})] \times h_3$$

with $[x_i]$ is the nearest integer to x_i, h_2 and h_3 are respectively Halton coefficient of base 2 and 3, In the end of this step we obtain a set of points S_L inside *RECT*. we used a mask *M* of *ROI* to get a subset S_I from S_L , this sets can be written as:

$S_L = \{p_1, p_2, \cdots, p_L\}$ where $p_i = (x_i, y_i)$ and

$$\begin{cases} x_{\min} \cdot x_i \langle x_{\max} \\ y_{\min} \cdot y_i \langle y_{\max} \end{cases}$$

$$\forall\ i = 1, 2, \ldots\ldots\ L$$

with $S_I = \{p'_1, p'_2, \cdots, p'_l\}$ where $p'_j \square S_I$ and $S_I \square S_L$

0.2.1 Seeds clustering

We employed a statistical method to partition the subset S_I into *k* classes denoted as C_i, where $i = 1, \ldots, k$. This clustering process enabled the creation of pixel subsets corresponding to distinct regions within our Region of Interest (*ROI*). To achieve this, we utilized the constrained k-means algorithm within a naive Bayesian framework [22]. Notably, this algorithm excels in providing optimal classification by incorporating neighboring pixel information. To further enhance the effectiveness of these classes, the constrained k-means algorithm initializes the parameter vector with the state *n*, and subsequently, we maximize the à posteriori probability to estimate the new state class parameters (*n* + 1).

0.2.2 K-Means Clustering

K-Means clustering is an unsupervised algorithm that is used to form different clusters of data sets so that they can be grouped together . A cluster is a collection of similar (homogeneous) data objects in one cluster and diverse (heterogeneous) data on objects in another cluster (see figure. 5). K-means is a clustering algorithm based on optimizing the criteria function. If the sample data is presented as aggregate $X = \{x_1, x_2, \ldots, x_n\}$, x_i is a d-dimensional vector, and suppose the number of clusters is *k*, the initial K-means center is $C_i(0)$. The similarity measurement adopts Euclidean istance, as for α and *β*.

$$D = [\alpha - \beta] = \sqrt{(\alpha - \beta)^T (\alpha - \beta)}$$

Grouping criteria adopt the number of squared errors.

$$J = \sum_{i=1}^{k} \sum_{x \in C_i} \left[x - C_i \right]^2$$

The steps in the K-Means clustering as follows:
1. Initialization of parameters: specify cluster *k* and center, initial K-Means $C_i(0)$ are specified as random data points, where $j = 1, 2, \ldots, k$.
2. Repeat revision: allocates each x_i data from the data set $X = \{x_1, x_2, \ldots, x_n\}$ to class $C_p(l)$ when:

$$\left\| x_i - C_p(l) \right\| < \left\| x_i - C_q(l) \right\|$$

Where *l* for iterations. $p, q = 1, 2, \ldots, n$, $p \neq q$, $l = 1, 2, \ldots, n$.
3. Update center cluster center: new cluster center on *l*+1 calculation

$$C_j(l+1) = \frac{1}{N_j} \sum_{x_i \in C_j(l)} x_i$$

Where N_j is the amount of data in the cluster *j*.
4. Stop the iteration if $C_i(l + 1) = C_i(l)$ or $|C_i(l +1)C_i(l)| < \epsilon$, if not repeat to step 2.

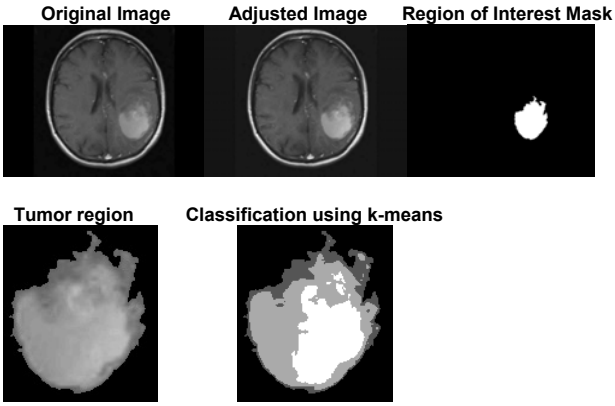

Fig. 3: Detection and classification process

0.3 Naive Bayes Classifier

To enhance the classification process, we utilize a Naive Bayes Classifier in conjunction with K-means. This combination demonstrates commendable performance when compared to other classifiers, owing to its simplicity, lower computational complexity, minimal memory demands, and strong predictive accuracy. The calculation of the Naive Bayes Classifier is delineated as follows (see figure. 4):

$$P(C_j | X) = \frac{P(X | C_i)\, P(C_i)}{P(X)}$$

Where, posterior probability, $P(C|X)$, is calculated using Class Prior Probability $P(C)$, Predictor Prior Probability $P(X)$ and Likelihood $P(X|C)$. The a posteriori estimation is achieved using iterated conditional mode [28]. The proposed method considers input data sets with attribute values as numerical and Gaussian distributions. For the Gaussian distribution the mean (μ) and standard deviation (σ) need to be calculated using the formula:

$$\mu = \frac{X_1 + X_2 + \ldots X_n}{n}$$

$$\sigma = \frac{\sum_{i=1}^{n} \left(X_i - \mu \right)^2}{n}$$

While the Gaussian distribution function is calculated by the formula:

$$f(X) = \frac{1}{2\pi\sqrt{\sigma}} \exp - \frac{(X - \mu)^2}{2\sigma^2}$$

The clustering process is considered as an initiator to our segmentation method. Each class must have an initial seed P_{seed_i}. Figure. 5, the initiator seed must verify this condition

$$\left| I\left(P_{seed_i} - m_i\right) \right| \min_{1 \langle j \langle l} \left\{ \left| I\left(P_j^i\right) - m_i \right| \right\}$$

with $I\left(P_j^i\right)$ is the pixel intensity of P_j^i

(a) (b)
(a) Tumor classification using classical Kmeans
(b) Tumor classification using constrained K-means

Fig. 4: MAP estimation of image classification using iterated conditional mode

0.3.1 Multi Segmentation

After selecting the initial seeds, the segmentation process for each class will be carried out using a modified region-growing method. The primary inconveniences associated with the classical region-growing approach are related to the selection of the initial seed and the homogeneity criteria, as noted by [9].

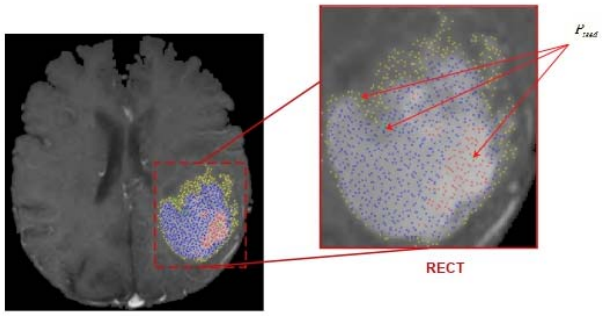

Fig. 5: distribution of points in *k* classes *k* = 3

The goal of the growth stage is to expand the region by incorporating neighboring pixels. This is achieved through a similarity measure that identifies connected pixels. Consequently, if the initial seed is placed in an area with significant inhomogeneity, the similarity measure may lead to substantial changes, potentially causing the growth process to halt prematurely. Thus, it is crucial to select starting points in the most homogeneous areas whenever possible.

On the other hand, a poor criterion could result in either only a partial region being covered or an excessively larger part than the region being included. Pixels are incorporated into the region based on the validity of the homogeneity criterion. To address this, we have initiated the segmentation process using an approach denoted as Pseedi for each class. To prevent overlaps between regions and maintain the integrity of segmented edges, gradient intensity information is utilized. For more comprehensive details about the segmentation process, please refer to Algorithm 1.

Algorithm 1 Algorithm: Segmentation process

Require: P_{seed_i} : initiator seed for classe i
C_i :pixels set allowed to classe i
$delta_{int}$: minimal intesity distance
$delta_{gradiene}$: minimal gradient distance
m_i :initiale average of classe i
G_{mi} :The gradient average of classe i
Ensure: R_i :Region i
Initialize the region R_i by the pixels assigned to the class
repeat
$V(P_{seed_i})$=neighborhood of P_{seed_i}
$border_{list} = border_{list} \cup V(P_{seed_i})$
Order $border_{list}$ in ascending order compared to $delta_{int}$.
P_{seed_i} = the first pixel of $border_{list}$ who check

$$[((I(p) - m_i) < delta_{int})\&\&$$

(Gradient(p)-G_{mi}) $< delta_{gradiene})$]**if** P_{seed_i} exist **then**
$R_i = R_i \cup P_{seed_i}$
$border_{list} = border_{list}(P_{seed_i})$
Update m_i
else
Break
end if
until P_{seed_i} not exist

Discussion and Experimental results

0.4 Materials and Database

We developed and tested our approach using Matlab 2018b as simulation software running on ubuntu 16.4 operating system, with cpu 2,20 GHz and processor intel core i7 with 8 GMb of Memory (RAM). We used 2 images from Brats Miccai 2015 database [20,21], which contain low-grade and hight-grade images of subjects segmented by radiologists into four sub-compositions of tumors.

0.5 Result and discussion

We used median filter to reduce the noise of the MRI images. Multi-segmenting was achieved using improved region growing methods initialized with constrained kmeans algorithm and Quasi Monte Carlo algorithms. The MRI images have been segmented into two regions, i.e., k equal to 2, in order to recognize two zones. These two classes correspond to edema (R1) and enhanced tumor (R2). Figure.6 (a,d) shows the MRI images of the open access database. Figure.6 (b,e) corresponds to the reference images made by the expert radiologist, and Figure6(c,f) represents the segmentation results using the method developed in this study.

In the aim to evaluate the performance of our approach. We use the confusion matrix. [17] to compute multiple Metrics in order to evaluate the performance of our approach, In order to measure the amount of overlap between the ground truth and our segmentation using three metrics (Dice, Sensitivity, Specificity) high value corresponds to a high level of overlap between the field and the reference.

$$Dice = \frac{2\,TP}{2\,TP + FP + FN}$$

$$Sensitivit\,y = TPR = \frac{TP}{TP + FN}$$

$$Specificit\,y = TNR = \frac{TN}{TN + FP}$$

where *TP*: true positive is the number of tumor pixels correctly detected, *TN*: true negative is the number of non tumor pixels correctly not detected, *FP*: false positive correspond to non-tumor pixels have been incorrectly detected as tumor pixels, *FN*: false negative is the number of non tumor pixels falsely detected. Thereafter, two metrics have been calculated, Hausdorff Distance (HD) and the mean minimum distance. Hausdorff Distance was calculated using the equation (see Table.2):

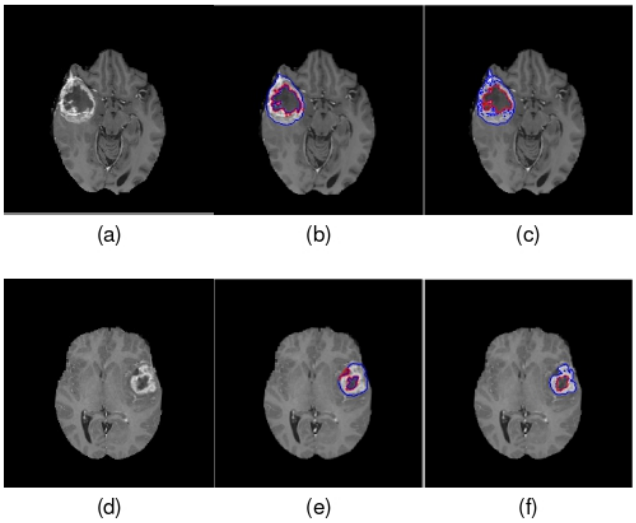

Fig. 6: (a,d): Original images, (b,e): segmentation of the expert, (c,f): segmented images using our approach.

HD(Distance Hausdorff) = *HD*(A,B)*max(h(a, b), h(b, a))*

with $h(a, b) = max_{a \in A}(min_{b \in B} ||a - b||)$
$AV\,D = max(d(A,B), d(B,A))$

Table 1. illustrates the accuracy and sensitivity performance of the method developed in this research. The results showed that dice changes in the range of 0.85 to 0.91 for Edema and from 0.77 to 0.84 for Enhanced tumor and the sensitivity changes in the range of 0.75 to 0.84 for Edema and from 0.64 to 0.65 for Enhanced tumor.

Table 1. Performance analysis of our method

	Dice		Sensitivity		Specificity	
images	R_1	R_2	R_1	R_2	R_1	R_2
1	90,12	71,35	80,25	54,92	100	99
2	89,73	82,14	80,54	68,55	100	99
3	91,44	76,90	84,28	63,80	100	99
4	90,12	71,54	81,35	55,43	100	98
5	85,38	75,14	75,92	65,34	98	98

Table 2. presents the range of Average Volume Difference (AVD) for both edema and enhanced tumor, which varies between 0.010 to 0. and 0.02 to 0.25, respectively. Additionally, the Hausdorff Distance (HD) ranges from 2 to 10.44 pixels for edema and 2.23 to 10 pixels for enhanced tumor. These results serve as strong evidence affirming the excellent performance of the automatic segmentation approach developed in this study.

Table 2. Distance analysis of the fully automatic segmentation approach

		Images					
		1	2	3	4	5	6
HD	R_1	3.7454	4.0125	5.1551	1.712	1.8021	8.5421
	R_2	9.8284	4,1126	2,0084	4,7541	2,9123	9,1191
AVD	R_1	0,1207	0,1018	0,0895	0,0951	0,0152	0,0954
	R_2	0,3251	0,0124	0,0124	0,0541	0,0184	0,1542

Table 3. displays the spatial performance outcomes achieved by our approach. These results closely align with those provided by experts, validating the efficacy of the fully automated segmentation approach developed herein. Furthermore, our findings underscore the significance of gradient information in reducing overlap between adjacent segmented regions. Notably, this technique exhibits rapid processing capabilities as it exclusively addresses areas of interest, obviating the need for tumor recognition training.

Table 3. Performance analysis of our method

		Dice (%)		**Sensitivity**(%)		**Specificity**(%)	
Authors	**Desription**	**Core**	**Enhanced**	**Core**	**Enhanced**	**Core**	**Enhanced**
Proposed work	QMC + Constrained Kmeans + RG	0.82	80,25	0.78	0.70	0.99	1
Hachemi [23]	QMC + EM + RG	0.80	0.71	0.72	0.57	0.9	0.8
Vaidhya [24]	Multimodal image + Autoencoder	0.68	0.64	0.66	0.74	0.71	0.53
Pereira [25]	CNN	0.76	0.73	0.90	0.72	0.86	0.81
Ellwaa [27]	Random orest + Iterative training	0.72	0.73	0.73	0.75	0.99	1
Demirhan [26]	wavelets + ANN	0.77	-	0.73	-	0.95	-

Conclusion

In conclusion, this study has successfully introduced a novel fully automatic multi-segmentation technique for brain tumor detection. Our approach involved a comprehensive series of image processing steps to enhance the quality of MRI images and accurately identify regions of interest. Specifically, we applied enhancement and denoising filters to preprocess

the MRI images, followed by the application of Kapur thresholding to isolate the regions of interest. For multi-segmentation, we employed an innovative approach by initializing the region-growing method with a hybrid technique combining K-means clustering with a Naive Bayesian approach. To further refine our results, we maximized the a posteriori probability through an Iterated Conditional Mode approach, and improved the region-growing process by incorporating a Quasi Monte Carlo sampling method. The outcomes of our study have demonstrated impressive performance, suggesting that our approach has the potential to replace conventional techniques for brain tumor detection. The combination of image enhancement, advanced segmentation, and probability maximization contributes to the robustness and accuracy of our method, making it a promising advancement in the field of medical image analysis

Authors: *Ph.D. Amina BAGDAOUI, Prof. Amina BENDAOUDI, Ph.D. Belkacem HACHEMI, Prof. Zouaoui CHAMA*
LEPO Laboratory,
Electronics Department,
Faculty of Electrical Engineering,
University o Djillali Liabes, BP. 89,
Sidi Bel Abbes, Algeria. Algeria

REFERENCES

[1] Alim-Ferhat, F and Boudjelal, A and Seddiki, S and Hachemi, B and Oudjemia, S.: Wavelet Energy Embedded into a Level Set Method for Medical Images Segmentation in the Presence of Highly Similar Regions, Mathematics and Computers in Sciences and in Industry (MCSI), 2014 International Conference on, IEEE, pp. 149–153, 2014.

[2] Anitha, R and Raja, D : Segmentation of glioma tumors using convolutional neural networks, International Journal of Imaging Systems and Technology, Wiley Online Library, 27(4), pp. 354–360, 2017.

[3] Cheng, Jun and Huang, Wei and Cao, Shuangliang and Yang, Ru and Yang, Wei and Yun, Zhaoqiang and Wang, Zhijianand Feng, Qianjin : Enhanced performance of brain tumor classification via tumor region augmentation and partition, PloS one, Public Library of Science, 10(10), pp. e0140381, 2015.

[4] Donoso, Ramiro and Veloz, Alejandro and Allende, Hector : Modified expectation maximization algorithm for MRI segmentation, Ibero american Congress on Pattern Recognition, Springer, pp. 63–70, 2010.

[5] El-Dahshan, El-Sayed A and Mohsen, Heba M and Revett, Kenneth and Salem, Abdel-Badeeh M : Computer-aided diagnosis of human brain tumor through MRI: A survey and a new algorithm, Expert systems with Applications, Elsevier, 41(11), pp. 5526–5545, 2014.

[6] Gordillo, Nelly and Montseny, Eduard and Sobrevilla, Pilar :State of the art survey on MRI brain tumor segmentation,

[7] Magnetic resonance imaging, Elsevier, 31(8), pp. 1426–1438, 2013.

[8] Kuwazuru, Jumpei and Arimura, Hidetaka and Kakeda, Shingo and Yamamoto, Daisuke and Magome, Taiki and Yamashita, Yasuo and Ohki, Masafumi and Toyofuku, Fukai and Korogi, Yukunori : Automated detection of multiple sclerosis candidate regions in MR images: false-positive removal with use of an ANN-controlled level-set method, Radiological physics and technology, Springer, 5(1), pp. 105–113, 2012.

[9] Lu, Xiaoqi and Wu, Jianshuai and Ren, Xiaoying and Zhang, Baohua and Li, Yinhui : The study and application of the improved region growing algorithm for liver segmentation,

[10] Optik-International Journal for Light and Electron Optics, Elsevier, 125(9), pp. 2142–2147, 2014.

[11] Maiti, Ishita and Chakraborty, Monisha : A new method for brain tumor segmentation based on watershed and edge detection algorithms in HSV colour model, Computing and Communication Systems (NCCCS), 2012 National Conference on, IEEE, pp. 1–5, 2012.

[12] Maitra, Madhubanti and Chatterjee, Amitava: Hybrid multiresolution Slantlet transform and fuzzy c-means clustering approach for normal-pathological brain MR image segregation, Medical Engineering and Physics, Elsevier, 30(5), pp. 615–623, 2008.

[13] Oliva, Diego and Cuevas, Erik and Pajares, Gonzalo and Zaldivar, Daniel and Perez-Cisneros, Marco : Multilevel thresholding segmentation based on harmony search optimization, Journal of Applied Mathematics, Hindawi, 2013, 2013.

[14] Rifai, Hilmi and Bloch, Isabelle and Hutchinson, Seth and Wiart, Joe and Garnero, Line : Segmentation of the skull in MRI volumes using deformable model and taking the partial volume effect into account, Medical image analysis, Elsevier, 4(3), pp. 219–233, 2000.

[15] Saritha, Saladi and Amutha Prabha, N : A comprehensive review: Segmentation of MRI images—brain tumor, International Journal of Imaging Systems and Technology, International Journal of Imaging Systems and Technology, 26(4), pp. 295–304, 2016.

[16] Somkantha, Krit and Theera-Umpon, Nipon and Auephanwiriyakul, Sansanee : Boundary detection in medical images using edge following algorithm based on intensity gradient and texture gradient features, IEEE transactions on biomedical engineering, IEEE, title=Boundary detection in medical images using edge following algorithm based on intensity gradient and texture gradient features, 58(3), pp. 567–573, 2011.

[17] Taha, Abdel Aziz and Hanbury, Allan : Metrics for evaluating 3D medical image segmentation: analysis, selection, and tool, BMC medical imaging, BioMed Central, 15(1), pp. 29–38, 2015.

[18] Weili, Shi and Yu, Miao and Zhanfang, Chen and Hongbiao, Zhang : Research of automatic medical image segmentation algorithm based on Tsallis entropy and improved PCNN,

Mechatronics and Automation, 2009. ICMA 2009. International Conference on, IEEE, pp. 1004–1008, 2009.
[19] Zhang, Yudong and Wu, Lenan : An MR brain images classifier via principal component analysis and kernel support vector machine, Progress In Electromagnetics Research, EMW Publishing, pp. 369–388, 2012.
[20] MICCAI BraTS Database 2015, [web page] http://braintumorsegmentation.org/, Nov. 20015.
[21] Menze, Bjoern H and Jakab, Andras and Bauer, Stefan and Kalpathy-Cramer, Jayashree and Farahani, Keyvan and Kirby, Justin and Burren, Yuliya and Porz, Nicole and Slotboom, Johannes and Wiest, Roland and others: The multimodal brain tumor image segmentation benchmark (BRATS), IEEE transactions on medical imaging, IEEE, 34(10), pp. 1993–2024, 2015.
[22] Z. Muda and Warusia, Mohamed and md, nasir, Sulaiman and Nur, Izura, Udzir : K-Means Clustering and Naive Bayes Classification for Intrusion Detection, Journal of IT in Asia, UNIMAS, 4(1), pp. 13–25, 2016.
[23] B. Hachemi and Z. Chama : Fully automatic multi-segmentation approach for magnetic resonance imaging brain tumor detection using improved region-growing and quasi-Monte Carlo expectation maximization algorithm, Int. J. Imaging Syst. Technol, Wiley, 30(1), pp. 104–111, 2020.
[24] K. Vaidhya and S. Thirunavukkarasu and V. Alex and G. Krishnamurthi : Multi-modal brain tumor segmentation using stacked Denoising autoencoders, Lecture Notes in Computer Science, Springer International Publishing, 30(1), pp. 181–194, 2016.
[25] S. Pereira and A. Pinto and V. Alves and CA. Silva : Brain tumor segmentation using convolutional neural networks in MRI images, IEEE Trans Med Imaging, IEEE, 35(5), pp. 1240–1251, 2016.
[26] A. Demirhan and M. Toru and I. Guler : Segmentation of tumor and edema along with healthy tissues of brain using wavelets and neural networks, IEEE J Biomed Health Inform, IEEE, 19(4), pp. 1451–1458, 2015.
[27] Brain Tumor Segmantation Using Random Forest Trained on Iteratively Selected Patients, [web page] https://www.springerprofessional.de/en/braintumorsegmantation using-random-forest-trained-on-iterativ/+, 2016. [Accessed on 23 March. 2019.].
[28] J. Besag : On the Statistical Analysis of Dirty Pictures, Journal of the Royal Statistical Society, serie B, 48(3), pp. 259–302, 1980.